*Present address: Transportation Systems Center (DOT), 55 Broadway, Cambridge, Mass. 02142.

[1]A. M. Ronn and David R. Lide, Jr., J. Chem. Phys. 47, 3669 (1967).

[2]T. Oka, J. Chem. Phys. 45, 752 (1966).

[3]T. Oka, J. Chem. Phys. 47, 13 (1967).

[4]T. Oka, J. Chem. Phys. 47, 4852 (1967).

[5]T. Oka, J. Chem. Phys. 48, 4919 (1968).

[6]T. Oka, J. Chem. Phys. 49, 3135 (1968).

[7]T. Shimizu and T. Oka, Phys. Rev. A 2, 1177 (1970).

[8]O. R. Wood and G. E. Schwarz, Appl. Phys. Letters 16, 518 (1970). See also M. Kovacs, D. Ramachandra Rao, and A. Javan, J. Chem. Phys. 48, 3339 (1968).

[9]B. Amme and S. Legvold, J. Chem. Phys. 30, 163 (1959). A further discussion will be found in our concluding remarks. For a review of kinetic studies see R. C. Millikan, Chem. Soc. (London) Spec. Publ. 20 (1966).

[10]C. Kittel, *Elementary Statistical Physics* (Wiley, New York, 1961), p. 156.

[11]The value of $\langle x^2 \rangle$ could be obtained from some averaging procedure such as $\langle x^2 \rangle = (1/4\pi AP)\int\int r^2 P_A dA\, d\Omega$, where A is the area of the cross section of the cell and r is the distance from the element dA to the wall along $d\Omega$. P is the laser power at dA. However, in view of our remarks on beam uniformity, this is not justified.

[12]L. Frenkel, S. Kryder, and A. A. Maryott, J. Chem. Phys. 44, 2616 (1966). Nonresonant cross sections closely follow viscosity values. We chose there because they form a consistent set for the mixtures used here.

[13]C. H. Townes and A. L. Schawlow, *Microwave Spectroscopy* (McGraw-Hill, New York, 1955), p. 76. The statistical weight $2J + 1$ is missing because the summation over initial states is usually included in the transition matrix element.

[14]In order to identify double-resonance signals we observed the spectra of several symmetrical-top molecules. Improved values of the rotation constants and more complete spectra will appear in J. Mol. Spectry. (to be published).

[15]E. W. Jones, R. J. L. Popplewell, and H. W. Thompson, Spectrochim. Acta 22, 669 (1966).

[16]T. M. Holladay and A. H. Nielsen, J. Mol. Spectry. 14, 371 (1964).

[17]A. Landman, H. Marantz, and V. Early, Appl. Phys. Letters 15, 357 (1969).

[18]K. M. Evenson, J. S. Wells, and L. M. Matarrese, Appl. Phys. Letters 16, 251 (1970).

Ion-Ion Mutual Neutralization Cross Sections Measured by a Superimposed Beam Technique. II. $O_2^+ + O_2^-$, $O_2^+ + NO_2^-$, and $NO^+ + NO_2^-$[†]

James R. Peterson, William H. Aberth, John T. Moseley,
and J. Roger Sheridan[*]

Stanford Research Institute, Menlo Park, California 94025

(Received 6 July 1970; revised manuscript received 30 November 1970)

Two-body ion-ion neutralization cross sections Q have been measured for $NO^+ + NO_2^-$ and $O_2^+ + NO_2^-$ and remeasured for $O_2^+ + O_2^-$. Using a superimposed-beams method, a range of barycentric energies between 0.15 and 200 eV was covered. The product $v_r Q$ behaved somewhat similarly for all reactants when plotted against the relative speed v_r. For relative energies above 3 eV, $v_r Q$ varies slowly and is of a magnitude of 10^{-7} cm^3/sec or greater. Below about 3 eV, however, $v_r Q$ begins to increase rather rapidly with decreasing energy, approaching the expected v_r^{-1} dependence. The low-energy data have been fitted to four-term polynomials in powers of v_r. In this form the data can be extrapolated to the thermal range and rate constants obtained. Reaction rates (300 °K) are given for the above reactants, and also for $H^+ + H^-$, $O^+ + O^-$, $N^+ + O^-$, and $N_2^+ + O_2^-$, which were studied earlier.

I. INTRODUCTION

The mutual neutralization of positive and negative ions by the reaction $A^+ + B^- \rightarrow A + B + \Delta E$ occurs in any ionized gas in which negative ions can be formed. Most practical interest in ion-ion mutual neutralization stems from its importance in the D region of the earth's ionosphere, where it terminates the negative-ion shuffle, and affects the relative concentrations of various ion species. [1,2] Theoretically, this type of reaction is of interest because the cross-section calculations based on curve-crossing models are relatively straightforward.

All published theoretical studies have been based on some form of a curve-crossing concept. For example, Magee,[3] Bates and Lewis,[4] Bates and Boyd,[5] and Olson *et al.*[6] have used the Landau-Zener approximation with varying degrees of sophistication, and Chan[7] has employed a WKB method to calculate electron tunneling in a model similar to curve crossing. Because of the long-range Coulomb attraction between the incident ions, the cross sections can be very large. These theories predict cross sections of a magnitude of 10^{-12} cm^2 at thermal energies, yielding rate coefficients in the 10^{-7}-cm^3 sec^{-1} range.

The first experimental approaches were limited

to the measurement of bulk electrical properties
of decaying plasmas, following ionization of alkali
metals in a flame[8] and of iodine and bromine vapors
in a pulsed rf discharge.[9] Reaction rates deduced
from these measurements ranged from about
5×10^{-9} to 2×10^{-8} cm^{3}sec^{-1}, but the values were
rather uncertain because of the indirectness of the
methods and the fact that the reacting ion species
were not determined. Mahan and co-workers[10,11]
later measured the properties of buffered-gas mix-
tures following ionization by vacuum uv photolysis.
They found rates for $NO^+ + NO_2^-$ in the low 10^{-7}-cm^3
sec^{-1} range at 300 °K, but again there was some
uncertainty about the identity of the reactants.
More recently, Hirsh and co-workers[12] have found
rates of about 5×10^{-8} for $NO^+ + NO_3^-$ and 2×10^{-7}
cm^3/sec for $NO^+ + NO_2^-$ by examining the decay of
mass-analyzed ions following the irradiation of
room temperature airlike mixtures by 1.5-MeV
electrons.

The development of the superimposed-beams
technique[13-15] ultimately has allowed the measure-
ment of cross sections for collisions between mass-
identified atomic and molecular reactants at well-
defined kinetic energies over a range extending
more than three orders of magnitude upward from
about 0.1 eV. In this technique, which has now
been applied to a variety of reactions, two beams
of atoms or molecules, typically at energies of
several keV in the laboratory frame of reference,
move together over a common path for a known
distance at variable relative velocities. Products
of reactions between the constituents of the two
beams are then separated from the beams and mea-
sured. The apparatus used in the measurements
reported here was first used to study $N^+ + O^- \rightarrow N + O$
reaction.[15] Subsequently, $N_2^+ + O_2^-$, $O_2^+ + O_2^-$,[16]
$H^+ + H^-$,[17] and $O^+ + O^-$[6] were examined. We report
here on the measurement of ion-ion neutralization
cross sections for $O_2^+ + NO_2^-$ and $NO^+ + NO_2^-$, which
are important species in the D region of the iono-
sphere. Because of the importance of these reac-
tions to upper atmospheric phenomena, we have
estimated their thermal reaction rates by first
fitting the low-energy data to a four-term polyno-
mial which approximates the low-energy behavior
predicted by Landau-Zener theory,[6] and then using
the resulting equation to perform Boltzmann averag-
ing in the thermal range. We have also reexamined
the low-energy behavior of the $O_2^+ + O_2^-$ reaction
because improvements in the apparatus and in its
operation suggested that the high degree of scatter
in the original data could be reduced and that ex-
trapolation to the thermal range could be made.

II. APPARATUS AND PROCEDURE

A detailed discussion of the apparatus and ex-
perimental technique has already been given.[16,17]

Briefly, positive- and negative-ion beams of differ-
ent speeds are merged by magnetic deflection, and
pass superimposed over a known path length (see
Fig. 1). Both beams have laboratory energies in
the keV range, but can have relative energies as
low as 0.15 eV while in the interaction region.
After they traverse the interaction length in super-
position, the beams are separated by electrostatic
deflection and collected in two Faraday cups. The
neutral particles formed by ion-ion neutralization,
as well as a much larger background of neutrals
formed by electron stripping and capture reactions
of the beam ions with the ambient gas, continue
along the superimposed beam direction and are
detected by secondary electron emission.

In order to separate the neutralization signal
from that due to beam-background gas interactions,
the positive and negative beams are electronically
chopped at 800 and 1000 Hz, respectively, and the
200-Hz beat component of the neutral signal is
measured. The signal that results when the beams
are demerged at the first set of deflectors (see
Fig. 1) is subtracted from the signal that results
when the beams flow superimposed to the second
set of deflectors, in order to obtain the signal due
to neutralization in the interaction region. This
signal is proportional to the product of the neutral-
ization cross section Q, and the relative speed v_r.

A number of improvements have been made in
the apparatus since it was discussed in Refs. 16
and 17. The effective mass resolution $m/\Delta m$ of
the beam merging magnet was limited at that time
to about 10 by the general optics of the apparatus.
During the production of the NO^+ beam from an
NO-gas discharge, however, both N_2^+ and O_2^+ are
also produced. The increased mass resolution of
better than 16 that is required to separate these
three species has been obtained by inserting a
Wien velocity filter (employing crossed electric
and magnetic fields) along the beam path between
the ion-source chamber and the intermediate
chamber (see Fig. 1 of Ref. 16). This filter,[18]
with suitable water cooling of its magnet, has in-
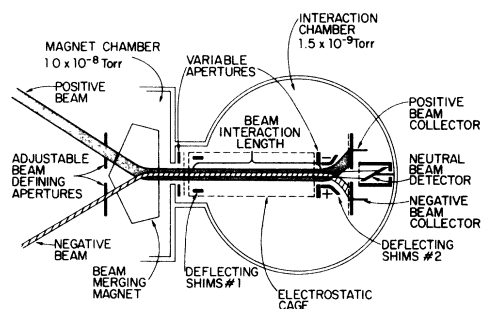
FIG. 1. Detailed schematic of the beam merging and
interaction regions.

creased the total resolution of the system to about 35. The N_2^+ and O_2^+ background contribution was thus reduced to below 2% of the NO^+ value. No similar resolution difficulties were experienced with the negative-ion beams.

An electrostatic cage that surrounds the beams over the length of the interaction region was also installed (see Fig. 1). It allows the relative energy of the merged beams to be varied without changing the energy and angle with which the beams enter the merging magnet. Thus application of a voltage V to the cage changes the relative difference in laboratory energies of the beams by 2 V. Use of the cage yields two advantages. First, a greater range of c.m. ion energies is now feasible. Second, data acquisition is more efficient since it is now possible to measure cross sections over a range of relative energies without the necessity of readjusting the angle with which one of the ion beams enters the merging magnet and without readjusting the focusing voltages. Cage voltages of greater than ± 400 V produce negligible effects on beam shapes or densities. The ion beams enter the electrostatic cage through a pair of 96% transparent tungsten wire mesh grids spaced 1 cm apart and oriented perpendicularly to the beam direction. The outer grid is grounded and the inner grid is at the cage potential. The inner grid is immediately followed by a pair of deflecting shims (shims No. 1 in Fig. 1). The deflecting shims are alternately maintained at the cage potential (undeflecting state) and ± 300 V relative to the cage (deflecting state). The difference in the neutral detector signals is then due only to positive-ion–negative-ion neutralization occurring along the bracketed length shown in Fig. 1. The beam exits the electrostatic cage through a 1.8-cm-diam opening (centered on the beam axis) which is ungridded to prevent the production of background neutrals by collisions of beam ions on the grid wires.

Each of the variable camera irises formerly positioned at the two ends of the interaction region[16] has been replaced with a combination of a large (1.3-cm-diam) fixed aperture and a small (0.3-cm-diam) aperture which can be moved in and out of the beam path by a pneumatic switch. This modification eliminates a previous 20% uncertainty in measuring beam current and density caused by uncertainty in the size of the iris aperture.

The barycentric energy W of merged ion beams of atomic masses M^+ and M^- with laboratory energies E^+ and E^- is given by

$$W = \tfrac{1}{2}\mu v_r^2 = \mu\left[(E^+/M^+)^{1/2} - (E^-/M^-)^{1/2}\right]^2 + \overline{W}_T, \quad (1)$$

where v_r is the relative speed between colliding particles, μ is the reduced mass, and $\overline{W}_T$ is the transverse energy contribution caused by imperfect collimation of the merged beams. Although direct

calculation of $\overline{W}_T$ is quite complicated and requires knowledge of parameters not measured in this research, its value can be estimated in several ways. Estimates of $\overline{W}_T$ from the collimator geometry[13] yield values in the range 0.05–0.25 eV.

Another method[17] of estimating $\overline{W}_T$ is based on knowledge of the character of the neutralization rate as a function of velocity at low velocity. As will be discussed, toward low velocities $v_r Q$ theoretically approaches a $1/v_r$ dependence for atomic ions. Thus use of too large a value for $\overline{W}_T$ yields low velocity values of $v_r Q$ that increase greater than $1/v_r$, which is not reasonable. For the atomic systems that we considered earlier ($H^+ + H^-$, $O^+ + O^-$, $N^+ + O^-$), it was observed that use of $\overline{W}_T = 0.2$ eV led to a $1/v_r$ dependence of $v_r Q$ at about 0.2 eV; use of $\overline{W}_T$ greater than 0.2 eV led to a faster increase. Therefore, an upper limit of 0.2 eV was set on $\overline{W}_T$.

A lower limit on $\overline{W}_T$ can be obtained in a similar way, since use of too small a value for $\overline{W}_T$ causes the slope of $\log_{10} v_r Q$ vs $\log_{10} v_r$ to decrease toward lower energies and prevents the extrapolation from ever reaching the $1/v_r$ dependence. Application of this criterion and variation of $\overline{W}_T$ in analysis of the data yielded a lower limit of $\overline{W}_T = 0.1$ eV for $H^+ + H^-$ and $N^+ + O^-$ and of 0.05 eV for $O^+ + O^-$.

Attempts to apply this type of analysis to determine the limits of $\overline{W}_T$ for the molecular systems were not successful. These systems apparently approach the $1/v_r$ dependence at lower energies than do the atomic systems, and thus this energy behavior is not as sensitive to variation of $\overline{W}_T$ in the energy range around 0.1 eV. A value of $\overline{W}_T = 0.15 \pm 0.05$ eV is therefore used for all the molecular systems, based on the limits obtained from the atomic systems.

The ion-ion neutralization signal is proportional to the product of the neutralization cross section Q and the relative speed v_r. This product is given by[16]

$$v_r Q = 2.69 \times 10^{-7} I_0 (E^+ E^-/M^+ M^-)^{1/2}$$
$$\times (4\Gamma J_A^* L\gamma)^{-1} \text{ cm}^3/\text{sec}. \quad (2)$$

In this expression, I_0 is the neutralization current at the neutral detector produced by secondary-electron emission; E^+ and E^- are in electron volts; γ is the effective neutral-particle secondary-electron emission coefficient; L is the interaction length, which for this experiment is 30 cm; Γ is the total negative beam current; and J_A^* is the current density of the (broad) positive beam in the region occupied by the (narrow) negative beam (see Fig. 1). Thus the overlap integral of the beams in the interaction region, $\int J^- J^+ dV$, is approximated by $J_A^* \Gamma L$.

III. ERROR CONSIDERATIONS

A description of the sources of error in this type

of merged-beam apparatus has been given earlier,[16] however, improvements in the apparatus have removed some of these sources and altered others. The following discussion is appropriate to the present apparatus.

The effective neutral-particle secondary-emission coefficient γ deserves careful consideration. The value assigned to γ is the average of γ^+ and γ^- that are experimentally determined for the positive- and negative-ion beams. When the electrostatic cage is grounded, and if it is assumed that the products of the neutralization are simply the neutral molecules of the interacting ions, this determination of γ is consistent with direct measurements of γ on other species and with observations,[16,19] that for beam energies of this experiment, γ changes only slightly for different charge states of a particle. For the ionic species considered here, it was observed that γ^- was larger than γ^+ by 10–15% between 2.6 and 4.0 keV. Since the neutral coefficient is expected to lie between the positive and negative ones, γ determined under these conditions should be accurate to within ±7%.

In general, however, the energies of the neutrals arriving at the detector are different from those of their parent ions used to determine γ^+ and γ^- as a result of the potential placed on the cage. Since γ is a function of the energy of the neutral particles arriving at the detector, an error could result from this energy difference. However, if the slopes of the secondary-emission coefficients as functions of energy are constant and the same for the positive and negative beams, the average γ will not be affected by equal and opposite changes in the energy of the two beams. The slope of the curves representing the secondary electron emission coefficients for O_2^+, NO^+, O_2^-, and NO_2^- ions are constant and the same to within 20% for the energies used in this experiment. We deduce that the error in γ due to this effect is ±3% for cage voltages up to ±700 V.

No analysis is made of the final products of the ion-ion neutralization reaction. It may be questioned whether different neutralization products will markedly affect the value of γ in Eq. (2). A plot was made of the secondary electron emission coefficient per unit mass versus velocity for NO_2^-, O_2^+, NO^+, O^-, and Q^+ over the velocity range of this experiment. The results of this plot indicate that all of the data fall on a straight line to within ±15%, showing the small expected variation with charge. These results are further substantiated by those of Tel'kovskii.[20] Since the velocities of the neutral products are the same as those of the parent ions inside the electrostatic cage, the average value of γ is essentially independent of the species in which the product neutrals appear.

From all of these considerations, we conclude

that the possible error in the value of $v_r Q$ induced by averaging γ^+ and γ^- to determine γ is ±10%.

A possible competing reaction with ion-ion neutralization is electron detachment

$$A^+ + B^- \rightarrow A^+ + B + e \ . \tag{3}$$
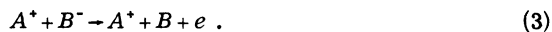
The electron affinity of NO_2 is about 2 eV, and this should also be the energy threshold for the electron-detachment reaction. For the relative-energy range of this experiment, Eq. (3) proceeds by means of two different curve crossings. The first crossing must bring the ionic system into a repulsive molecular state that can then cross into an electron-detachment state. This type of reaction, which requires a crossing from a repulsive state, can only occur for impact parameters less than about 3 Å. Such reactions must therefore have maximum cross sections less than about 10^{-15} cm^2, and are negligible compared to the mutual neutralization cross sections.

This approximation used to determine the overlap integral leads to an uncertainty of ±20%. An uncertainty in the interaction length L is present because the beams are not demerged instantaneously at the second pair of deflectors. In fact, they emerge from the electrostatic cage a short distance before reaching the deflectors. The 30-cm effective length for L is uncertain by ±8%. The ion-ion neutralization current I_0 is determined by recording the output of the lock-in amplifier for periods up to 5 min and then averaging the signal obtained. For the data presented here, this determination could always be made to within ±15% and often to within ±5%. Thus error limits of ±10% are placed on I_0. As has been discussed, the measurement of γ is uncertain by ±10%. Other error contributions are small. I^- is determined to within ±4%, J_A^+ to ±6%, and E^+ and E^- to ±1%. The rms error determined from these individual uncertainties is ±27%. This is in good agreement with the observed scatter of the data about the fitted curves.

IV. RESULTS AND DISCUSSION

The results of the measurements of $O_2^+ + NO_2^-$, $NO^+ + NO_2^-$, and $O_2^+ + O_2^-$ are shown in Figs. 2–4. For convenience in deducing the rate-constant behavior, the data are plotted as the product $v_r Q$ vs v_r, where v_r is the relative speed of the interacting ions and Q is the neutralization cross section. Similar to previous measurements on other systems,[16,17] the values of $v_r Q$ are near 10^{-7} cm^3/sec, but show quite different velocity dependencies from one another. The $O_2^+ + NO_2^-$ data (Fig. 2) fall rapidly to about 1.5×10^{-7} cm^3/sec at 3 eV, remain almost constant at that value out to about 40 eV, and then rise slowly. The $NO^+ + NO_2^-$ data (Fig. 3) decrease rapidly out to 3 eV, then more slowly

BARYCENTRIC ENERGY —— eV
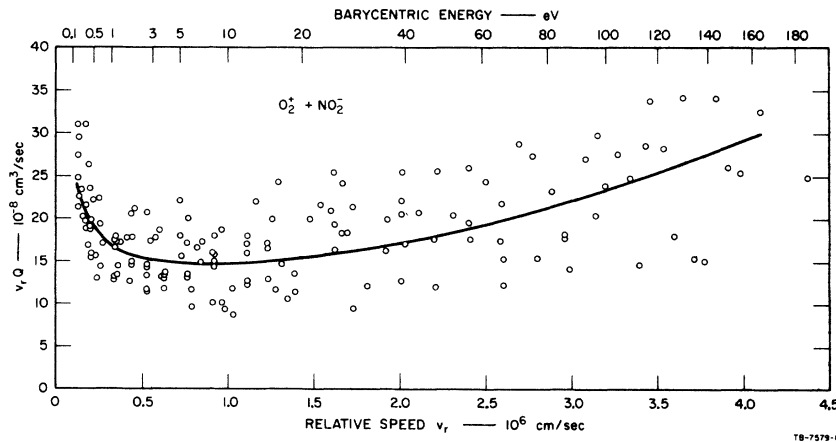
FIG. 2. Neutralization-rate measurements versus relative velocity for $O_2^+ + NO_2^-$. The solid curve represents a least-squares fit of the data points to the functional form $v_r Q = A/v_r + B + Cv_r + Dv_r^2$.

over the remainder of the observed energy range. The $NO^+ + NO_2^-$ results are smaller than both the $O_2^+ + O_2^-$ and the $O_2^+ + NO_2^-$ results over most of the energy range considered, but they rise rapidly at low energies to give the largest thermal-energy-rate coefficient that we have determined to date.[15-17]

Figure 4 shows the present $O_2^+ + O_2^-$ data (circles and solid line) and also the average of the previously published data (dashed line). The earlier data contained a high degree of scatter which masked the increase in $v_r Q$ toward lower energies below 10 eV. This increase is readily apparent in the present data. The noise in the early data apparently was produced by arcing in the positive-ion source. This arcing not only produced instability in the O_2^+ beam but a recent investigation showed that it also altered the gain characteristics of the lock-in am-

plifier. In the present measurements, readjustment of the spacing between the source anode and extracting lens, careful monitoring of the O_2-source gas-pressure, and frequent cleaning of both the anode and extracting electrode prevented the arcing that had upset the earlier measurements.

The solid curves of Figs. 2–4 represent a least-squares fit of the data to the functional form

$$v_r Q = A/v_r + B + Cv_r + Dv_r^2. \tag{4}$$

Using the Landau-Zener formulation,[4,5] it can be shown[6] that $v_r Q$ will be dominated by a v_r^{-1} dependence at very low energies, and that as the energy is increased, the dependence will depart from v_r^{-1} in the manner described by Eq. (4). Thus Eq. (4) can be viewed as a low-energy expansion of the appropriate Landau-Zener formula, but the func-

BARYCENTRIC ENERGY —— eV
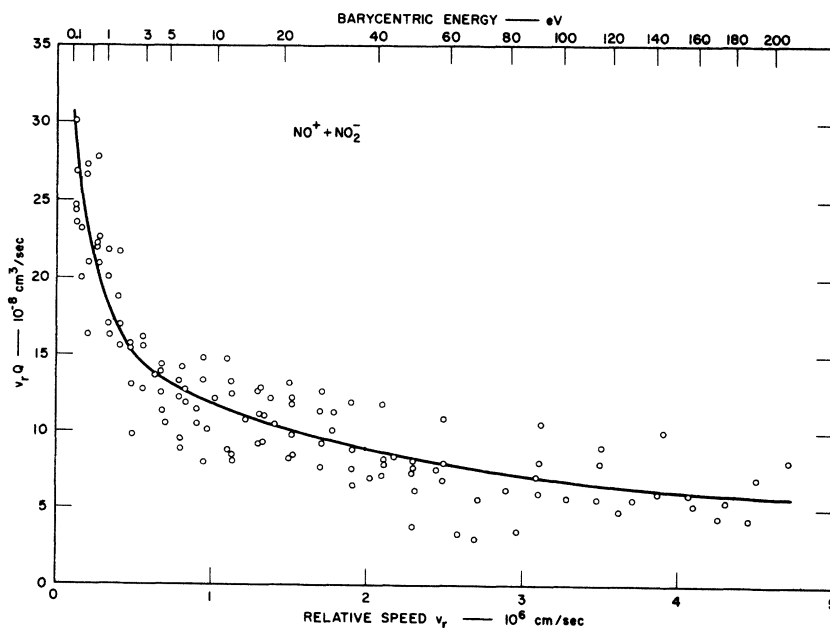
FIG. 3. Neutralization-rate measurements versus relative velocity for $NO^+ + NO_2^-$. The solid curve represents a least-squares fit of the data points to the functional form $v_r Q = A/v_r + B + Cv_r + Dv_r^2$.
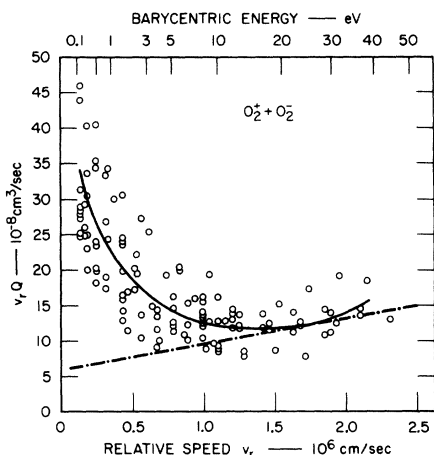
FIG. 4. Neutralization-rate measurements versus relative velocity for $O_2^+ + O_2^-$. The solid curve represents a least-squares fit of the data points to the functional form $v_r Q = A/v_r + B + C v_r + D v_r^2$. The dashed curve is the average of previously published (Ref. 16) experimental results.

tional form of Eq. (4) permits easy calculation of the thermal-rate coefficient $\alpha(T)$ from the equation

$$\alpha(T) = (2/\pi)^{1/2} (\mu/kT)^{3/2} \int Q(v_r) v_r^3 \, e^{-\mu v_r^2/2kT} \, dv_r .$$

(5)

Integration of Eq. (5) yields

$$\alpha(T) = (2\mu/\pi kT)^{1/2} A + B + (8kT/\mu\pi)^{1/2} C + (3kT/\mu) D .$$

(6)

Equation (6) can now be used as the basis for extrapolating the thermal-rate coefficient down to 300 °K and below. Because of their importance to studies of ionized gases occurring naturally or in the laboratory, we have calculated thermal rates from low-energy extrapolations of the data for the reactions reported here, and also for all other reactions that we have studied. Table I gives the resultant rates at 300 °K. Also included in the table are the values of the coefficients used in the extrapolation.

These can be used to obtain rates at other temperatures.

The estimated error limits assigned to the rates in Table I represent our best estimate of approximately 70% confidence limits. They include the combined uncertainties in the measurements plus the uncertainties in extrapolating the data to thermal energies, due to the indefiniteness in the value of $\overline{W}_T$.

The semiclassical theory used by Chan[7] to calculate the reaction rate for the process $O_2^+ + O_2^- \to O_2 + O + O$ yielded 1.14×10^{-7} cm^3/sec at 300 °K and indicated that this dissociative channel dominates the neutralization. This result is approximately a factor of 4 lower than our determination of 4.2×10^{-7} cm^3/sec for the total neutralization rate, $O_2^+ + O_2^- \to$ neutrals.

It is immediately evident from Table I that the A coefficients used for the thermal-rate extrapolation are larger relative to the B coefficients for the atomic reactions than for the molecular ones. As mentioned above, the low-energy behavior of $v_r Q$ is expected to approach a $1/v_r$ slope as the barycentric energy falls below ΔE, the exothermic energy of the reaction.[4,5] The difference in the A/B ratios for molecules and atoms may reflect a smaller value of ΔE for the molecules due to the existence of vibrational energy levels which increase the number of final states available in the reactions.

The cross sections measured here all show the general characteristics that are expected for the ion-ion neutralization reaction. At high velocities v_r, the product $v_r Q$ is not strongly dependent on velocity. However, at low v_r, as the relative energy approaches 0.1 eV, there is a rather steep rise, and $v_r Q$ goes toward the v_r^{-1} dependence predicted for atomic systems. Beyond these general characteristics, each reactant pair has its own peculiar cross-section curve, reflecting the different intermolecular forces and arrangements of electronic states in each system.

Extrapolations of the low-energy data lead to thermal-rate constants which exceed 4×10^{-7} cm^3/sec at 300 °K. These data thus indicate that the

TABLE I. Calculated thermal rates from low-energy extrapolations and associated parameters.

Reaction	Data range 0.15 (eV)	$10^2 A$ (cm^4/sec^2)	$10^8 B$ (cm^3/sec)	$10^{14} C$ (cm^2)	$10^{20} D$ (cm/sec)	$10^8 \alpha$ (300 °K) (cm^3/sec)
$H^+ + H^-$	20	9.18	6.26	-0.448	0.089	39 ± 21
$O^+ + O^-$	20	1.75	2.70	-0.505	5.09	27 ± 13
$N^+ + O^-$	20	1.57	4.14	3.34	-0.547	26 ± 8
$O_2^+ + O_2^-$	13	0.460	35.1	-45.5	21.7	42 ± 13
$N_2^+ + O_2^-$	100	0.287	10.4	0.396	0.143	16 ± 5
$NO^+ + NO_2^-$	20	1.54	18.2	-15.7	7.19	51 ± 15
$O_2^+ + NO_2^-$	20	1.24	14.3	-3.58	2.22	41 ± 13

values of 1 to $2 \times 10^{-7} \, cm^3/sec$ normally assumed for ion-ion mutual neutralization rates in ionospheric models are too small by at least a factor of 2. This conclusion is, however, subject to the following considerations.

The merged-beam technique affords an accurate control over the identity of the atoms and molecules that take part in the reactions, and of their relative energies over a very large dynamic range. However, as is the case in many fast-beam experiments there is some uncertainty in the internal states of the beam particles, particularly when the species have metastable electronic states. In order to be present as the beams enter the interaction region in our apparatus, the excited states must live for at least $5 \times 10^{-6} \, sec$. Little is known about the probability of forming excited electronic states in O_2^- and NO_2^-; however, such states may exist, and furthermore the molecules can be vibrationally excited. Studies of O_2^+ and NO^+ ion beams produced by electron bombardment[21,22] indicate that the production of metastable states becomes significant at a few eV above threshold. From qualitative considerations, it would appear that a reduction in the binding energy of the attached electron, caused by vibra-

tional and electronic excitation of the negative ion, would tend to increase the neutralization cross section. Similar excitations in the positive ions probably would not have as strong an effect on the neutralization reaction. During the course of this experiment we made some attempts to influence the neutralization cross section by changing the positive-ion source conditions (thus changing the percentage metastable population); however, the tests yielded no effect. Neither the vibrational nor the electronic populations of the positive- or negative-ion beams were monitored. If our beams contained substantial fractions of excited states (particularly in the negative beams), the present measurements may show larger cross sections than would be found with completely unexcited ions of the same species. Future efforts will be directed towards monitoring the excitation populations of the reacting ions and examining their effects on the neutralization cross sections.

ACKNOWLEDGMENTS

†Work sponsored by the Defense Atomic Support Agency Reaction Rate Program through Air Force Cambridge Research Laboratories.

*Present address: Physics Department, University of Alaska, College, Alas. 99701.

[1]R. E. LeLevier and L. M. Branscomb, J. Geophys. Res. Space Phys. 73, 27 (1968).

[2]F. E. Niles, J. Chem. Phys. 52, 408 (1970).

[3]J. L. Magee, Discussions Faraday Soc. 12, 33 (1952).

[4]D. R. Bates and J. T. Lewis, Proc. Phys. Soc. (London) A68, 173 (1955).

[5]D. R. Bates and T. J. M. Boyd, Proc. Phys. Soc. (London) A69, 910 (1956).

[6]R. E. Olson, J. R. Peterson, and J. T. Moseley, J. Chem. Phys. 53, 3391 (1970).

[7]F. T. Chan, J. Chem. Phys. 45, 2540 (1958).

[8]P. F. Knewstubb and T. M. Sugden, Trans. Faraday Soc. 54, 372 (1958).

[9]T. H. Y. Yeung, Proc. Phys. Soc. (London) 71, 341 (1958).

[10]B. H. Mahan and J. C. Person, J. Chem. Phys. 40, 392 (1964).

[11]T. S. Carleton and B. H. Mahan, J. Chem. Phys.

40, 3683 (1964).

[12]M. N. Hirsch (private communication).

[13]S. M. Trujillo, R. H. Neynaber, and E. W. Rothe, Rev. Sci. Instr. 37, 1655 (1966).

[14]V. A. Belyaev, B. G. Brezhnev, and E. M. Erastov, Zh. Eksperim. i Teor. Fiz. 52, 1170 (1967) [Sov. Phys. JETP 25, 777 (1967)].

[15]W. Aberth, J. R. Peterson, D. C. Lorents, and C. J. Cook, Phys. Rev. Letters 20, 979 (1968).

[16]W. H. Aberth and J. R. Peterson, Phys. Rev. A 1, 158 (1970).

[17]J. Moseley, W. Aberth, and J. R. Peterson, Phys. Rev. Letters 24, 435 (1970).

[18]Model 300 Wien Filter, manufactured by Colutron Corp., Boulder, Colo.

[19]H. C. Hayden and N. G. Utterback, Phys. Rev. 135, A1575 (1964); E. S. Chambers, ibid. 133, A1202 (1964).

[20]V. G. Tel'kovskii, Dokl. Akad. Nauk SSSR 108, 444 (1956) [Sov. Phys. Doklady 1, 334 (1956)].

[21]B. R. Turner, J. A. Rutherford, and D. M. J. Compton, J. Chem. Phys. 48, 1602 (1969).

[22]R. F. Mathis, B. R. Turner, and J. A. Rutherford, J. Chem. Phys. 49, 2051 (1969); 50, 2270 (1969).

FIG. 1. Detailed schematic of the beam merging and interaction regions.